The Journal of Immunology

Shear Stress–Dependent Downregulation of the Adhesion-G Protein–Coupled Receptor CD97 on Circulating Leukocytes upon Contact with Its Ligand CD55

Olga N. Karpus, Henrike Veninga, Robert M. Hoek, Dennis Flierman, Jaap D. van Buul, Corianne C. vandenAkker, Ed vanBavel, M. Edward Medof, René A. W. van Lier, Kris A. Reedquist and Jörg Hamann

J Immunol 2013; 190:3740-3748; Prepublished online 27 February 2013;
doi: 10.4049/jimmunol.1202192
http://www.jimmunol.org/content/190/7/3740

The Journal of Immunology is published twice each month by
The American Association of Immunologists, Inc.,
1451 Rockville Pike, Suite 650, Rockville, MD 20852

Print ISSN: 0022-1767 Online ISSN: 1550-6606.

Shear Stress–Dependent Downregulation of the Adhesion-G Protein–Coupled Receptor CD97 on Circulating Leukocytes upon Contact with Its Ligand CD55

Olga N. Karpus,*[,1] Henrike Veninga,*[,1] Robert M. Hoek,* Dennis Flierman,* Jaap D. van Buul,[†] Corianne C. vandenAkker,[‡] Ed vanBavel,[§] M. Edward Medof,[¶] René A. W. van Lier,* Kris A. Reedquist,* and Jörg Hamann*

Adhesion G protein–coupled receptors (aGPCRs) are two-subunit molecules, consisting of an adhesive extracellular α subunit that couples noncovalently to a seven-transmembrane β subunit. The cooperation between the two subunits and the effect of endogenous ligands on the functioning of aGPCRs is poorly understood. In this study, we investigated the interaction between the pan-leukocyte aGPCR CD97 and its ligand CD55. We found that leukocytes from CD55-deficient mice express significantly increased levels of cell surface CD97 that normalized after transfer into wild-type mice because of contact with CD55 on both leukocytes and stromal cells. Downregulation of both CD97 subunits occurred within minutes after first contact with CD55 in vivo, which correlated with an increase in plasma levels of soluble CD97. In vitro, downregulation of CD97 on CD55-deficient leukocytes cocultured with wild-type blood cells was strictly dependent on shear stress. In vivo, CD55-mediated downregulation of CD97 required an intact circulation and was not observed on cells that lack contact with the blood stream, such as microglia. Notably, de novo ligation of CD97 did not activate signaling molecules constitutively engaged by CD97 in cancer cells, such as ERK and protein kinase B/Akt. We conclude that CD55 downregulates CD97 surface expression on circulating leukocytes by a process that requires physical forces, but based on current evidence does not induce receptor signaling. This regulation can restrict CD97–CD55-mediated cell adhesion to tissue sites. ***The Journal of Immunology*****, 2013, 190: 3740–3748.**

The adhesion class is one of the five classes of G protein–coupled receptors (GPCRs) (1). The human genome encodes 33 adhesion GPCRs (aGPCRs), which are broadly expressed in embryonic and larval cells, cells of the reproductive tract, neurons, leukocytes, and a variety of tumors (2). Most notable is the molecular structure that sets aGPCRs apart from other GPCRs. Intramolecular processing at a GPCR-proteolytic site (GPS) proximal to the first transmembrane helix gives rise to an extracellular α-subunit and a seven-transmembrane β-subunit, which subsequently reassociate noncovalently (3). Recently it became clear that the GPCR-proteolytic site motif is part of a much larger, ∼320-residue GPCR autoproteolysis-inducing (GAIN) domain that forms a tightly associated heterodimer upon proteolysis (4).

The extracellular subunits of aGPCRs can be exceptionally long and contain a variety of structural domains that are known for their ability to facilitate cell-cell and cell-matrix interactions. The first ligand identified was CD55, a widely distributed cell surface molecule regulating complement activity (decay-accelerating factor) (5). CD55 interacts with the N-terminal epidermal growth factor (EGF)-like domains of CD97 (6–8), an aGPCR broadly expressed by hematopoietic and nonhematopoietic cells (9–11). Subsequently identified aGPCR ligands were dermatan sulfate, α5β1 integrin, tissue transglutaminase 2, phosphatidylserine, LPS, C1q, lasso/teneurin-2, collagen III, and Thy-1/CD90 (12–20). Evidence was obtained that aGPCRs have a role in cell positioning and tissue organization in various organ systems (21, 22); however, in the strictest sense, aGPCRs are still functional orphans. The main problem is a lack of understanding of how these atypical GPCRs are activated. For classical GPCRs, ligand binding results in the formation of a transient high-affinity complex of agonist, activated receptor, and G protein. As a consequence, GDP is released from the G protein and replaced by GTP, leading to dissociation of the G protein into an α subunit and a βγ dimer, which both activate several effectors (23). For aGPCRs, the agonistic potential of most ligands is uncertain. Studies on signal transduction have been done almost exclusively in the absence of agonists and have not revealed a general mechanism of action (2). This uncertainty has fostered the idea that aGPCRs function in a principally different manner from classical GPCRs (5th Workshop on Adhesion-GPCRs, May 1, 2010, Leipzig, Germany, www.adhesiongpcr.org).

In this study, we used the CD97–CD55 interaction as a paradigm to explore the consequences of ligation of an aGPCR both

*Department of Experimental Immunology, Academic Medical Center, University of Amsterdam, 1105 AZ, Amsterdam, The Netherlands; [†]Sanquin Research and Landsteiner Laboratory, Department of Molecular Cell Biology, Academic Medical Center, University of Amsterdam, 1066 CX Amsterdam, The Netherlands; [‡]Biological Soft Matter Group, Fundamental Research on Matter Institute for Atomic and Molecular and Physics, 1098 XG Amsterdam, The Netherlands; [§]Department of Biomedical Engineering and Physics, Academic Medical Center, University of Amsterdam, 1105 AP Amsterdam, The Netherlands; and [¶]Institute of Pathology, Case Western Reserve University, Cleveland, OH 44106

[1]O.N.K. and H.V. contributed equally to this work.

Received for publication August 7, 2012. Accepted for publication January 28, 2013.

This work was supported by the Netherlands Organisation for Scientific Research (NWO 814.02.012), the Dutch Arthritis Association (DAA 0701022), and the Landsteiner Foundation for Blood Transfusion Research (LSBR 0310).

Address correspondence and reprint requests to Dr. Jörg Hamann, Department of Experimental Immunology, Room K0-140, Academic Medical Center, University of Amsterdam, P.O. Box 22700, 1100 DE Amsterdam, The Netherlands. E-mail address: j.hamann@amc.uva.nl

Abbreviations used in this article: aGPCR, adhesion GPCR; EGF, epidermal growth factor; GKN, glucose–potassium–sodium buffer; GPCR, G protein–coupled receptor; PBLk, peripheral blood leukocyte; PKB, protein kinase B; sCD97, soluble CD97.

www.jimmunol.org/cgi/doi/10.4049/jimmunol.1202192

in vivo and in vitro. We demonstrate that CD55 contact leads to a continuous downregulation of CD97 on circulating leukocytes that is dependent on physical shear stress and can serve to restrict CD97-mediated cell adhesion to tissue sites. De novo contact of $CD97^+$ leukocytes with CD55 did not appear to induce signaling pathways that were recently shown to be constitutively activated by CD97 in cancers cells (24). To our knowledge, our findings demonstrate for the first time the interaction of an aGPCR with an endogenous ligand in vivo and support the hypothesis that facilitating adhesive contacts may be a prime activity of the extracellular modules of aGPCRs.

Materials and Methods

Mice

Mice deficient for CD55 (*Cd55*$^{-/-}$; synonym: *Daf1*$^{-/-}$) and CD97 (*Cd97*$^{-/-}$) have been generated previously by us (25, 26) and backcrossed to C57BL/6 for at least eight generations. Wild-type mice were littermates or were purchased from Charles River (Maastricht, The Netherlands). Congenic mice expressed *Cd45.1* in the B6.SJL strain. All mice used in this study were matched for age and sex and kept under specific pathogen-free conditions. Experiments were approved by the Animal Ethics Committee of the Academic Medical Center (Amsterdam, The Netherlands).

Adoptive transfer

The equivalent of 25×10^6 congenic wild-type (*Cd45.1*) or *Cd55*$^{-/-}$ (*Cd45.2*) leukocytes, obtained by mashing the spleens under aseptic conditions in sterile PBS through a 70-μm cell strainer, were injected into the tail vein of *Cd55*$^{-/-}$ or congenic wild-type recipient mice, respectively. To allow tracing of *Cd55*$^{-/-}$ splenocytes transferred into *Cd55*$^{-/-}$ mice, cells were labeled prior to the injection with 1 μM CFSE (Molecular Probes, Leiden, The Netherlands) for 10 min at 37°C. To block coagulation in vivo, 20 U/ml heparin (LEO Pharma, Breda, The Netherlands) in PBS was injected into the tail veins of mice 5 min before the injection of *Cd55*$^{-/-}$ splenocytes. At various times, blood and spleen from recipient mice were collected and analyzed by flow cytometry and Western blotting for CD97 expression on leukocytes. For Western blot analysis, CFSE-positive transferred leukocytes were sorted on a FACSAria (BD Biosciences, San Jose, CA) into PBS.

Bone marrow–chimeric mice

Congenic wild-type (*Cd45.1*) and *Cd55*$^{-/-}$ (*Cd45.2*) recipient mice were irradiated with 5.1 Gy γ radiation and reconstituted with 10×10^6 *Cd55*$^{-/-}$ or congenic wild-type bone marrow–derived hematopoietic cells, respectively, via tail vein injection. Mice were housed in individually ventilated cages and obtained drinking water containing neomycin during the experiment. After 5 wk, blood was collected in heparin via heart puncture and analyzed by flow cytometry for CD97 expression on leukocytes.

Coculture assays

To mimic shear stress in vitro, 100 μl congenic wild-type or *Cd55*$^{-/-}$ whole blood was added to 2.5×10^6 *Cd55*$^{-/-}$ or wild-type splenocytes in polypropylene tubes and shaken at RT at 900 rpm or not agitated. At indicated times, cells were harvested and analyzed by flow cytometry for CD97 expression. Alternatively, 500 μl congenic wild-type whole blood was mixed with 12.5×10^6 *Cd55*$^{-/-}$ splenocytes and exposed at 25°C to shear stresses of 1 dyne/cm^2, resembling capillary levels (27), or 40 dyne/cm^2, representative for arterial shear stresses in mice (28), imposed by a rheometer (MCR 501; Anton Paar, Graz, Austria). After 1 h, cells were harvested and analyzed by flow cytometry for CD97 expression.

To study potential signaling after de novo ligation of CD97 by its ligand CD55, 10×10^6 *Cd55*$^{-/-}$ or wild-type splenocytes were mixed with a leukocyte-free fraction of *Cd55*$^{-/-}$ or wild-type erythrocytes, obtained by filtering wild-type whole blood diluted in PBS through a filter, containing two layers of prefilter material (#S3AT0006) and three layers of intermediate material (#2210; Fresenius Kabi, Isola della Scala, Italy). After applying shear stress to the mixed cells for 0, 5, 15, or 30 min, erythrocytes were lysed with a buffer containing 155 mM NH_4Cl, 10 mM $KHCO_3$, and 1 mM EDTA, and the remaining splenocytes were washed in PBS and collected in radioimmunoprecipitation assay buffer (Cell Signaling, Beverly, MA) for biochemical analysis. *Cd55*$^{-/-}$ splenocytes stimulated with 100 ng/ml PMA for 5 or 15 min were used as positive controls.

Immunologic reagents

For flow cytometry, a hamster mAb against the first EGF domain of CD97 (clone 1B2) (29, 30) was used with an irrelevant hamster control mAb (clone 3C7). Abs were biotinylated in house and used in combination with streptavidin-conjugated PeCy7 or allophycocyanin, and FITC-, PE-, PerCP-Cy5.5-, PeCy7-, allophycocyanin-, or biotin-conjugated mAbs specific for CD3, CD11b, CD45, CD45.1, CD45.2, CD62L, B220, F4/80, Gr-1, Ly6C, NK1.1 (all from eBioscience, San Diego, CA, USA), Ly6G (BD Biosciences), annexin V (IQ Products BV, Groningen, The Netherlands). For Western blot analysis, we used polyclonal Abs against the α-chain of CD97 (R&D Systems, Wiesbaden, Germany), the β-chain of CD97 (26), phospho-ERK, ERK, phospho-Akt, and actin (all from Cell Signaling).

Flow cytometry

Bone marrow cells were harvested from dissected femurs by flushing the bone marrow plug with PBS/0.5% BSA. Peripheral blood was collected in heparin by heart puncture. Single-cell suspensions of spleen were obtained as described above. Erythrocytes in all cell preparations were lysed as described above.

For microglia isolation (31), brains were transferred to ice-cold glucose–potassium–sodium buffer (GKN; 8 g/l NaCl, 0.4 g/l KCl, 1.77 g/l $Na_2HPO_4 0.2H_2O$, 0.69 g/l $NaH_2PO_4.H_2O$, 2 g/l D-(+)-glucose, pH 7.4) with 0.3% BSA and minced through a 70-μm cell strainer. Cells were washed and resuspended in 20 ml isotonic Percoll (GE Healthcare, Zeist, The Netherlands), diluted in GKN/BSA to a density (ρ) of 1.03 g/ml, then underlain with 10 ml Percoll (ρ = 1.095), overlain with 5 ml GKN-BSA buffer, and centrifuged for 35 min at 2500 rpm ($1335 \times g$) and 4°C with slow acceleration and no brake. After discarding of the myelin layer on top of the Percoll phase (ρ = 1.03), cells were collected from the interface, washed, and resuspended in GKN/BSA buffer.

Whole blood (50 μl), 5×10^5 bone marrow or spleen cells, or all microglial cells isolated from one brain were used per staining. Nonspecific binding of mAbs was blocked by adding 10% normal mouse serum and 2.5 μg/ml anti-CD16/32 (clone 2.4G2; BD Biosciences), together with the appropriately diluted mAbs in PBS containing 0.5% BSA. Cells were incubated for 30 min at 4°C, followed (when appropriate) by a second incubation step with streptavidin-FITC, -PeCy7, or -allophycocyanin. For measuring viability, cells were washed in calcium buffer (10 mM HEPES, 150 mM NaCl, 5 mM KCl, 1 mM $MgCl_2$, 2.5 mM $CaCl_2$) and stained for annexin V in combination with subset-specific cell markers. Flow cytometric analysis was performed using a FACSCalibur (BD Biosciences) and the FlowJo software package (Tree Star, Ashland, OR).

Western blot analysis

Immune cells from spleen and blood or CFSE-positive transferred cells from blood were isolated as described above and solubilized in a lysis buffer consisting of 2% Triton X-100 in PBS, supplemented with Complete Protease Inhibitor Mix (Roche, Mannheim, Germany). Lysates were made by agitation for 30 min at 4°C, after which insoluble material was removed by centrifugation in a microfuge at $16{,}100 \times g$ for 15 min. The resulting supernatant was used for SDS-PAGE. Approximately 3×10^6 cell equivalents were loaded on a protein gel and blotted to an Immobiolon-FL polyvinylidene fluoride membrane (Millipore, Bedford, MA) by semidry blotting. Membranes were stained overnight using Abs specific for the CD97 α- and β-chain, phospho-ERK, ERK, phospho-Akt, and actin. For detection, IRDye-tagged secondary Abs (LI-COR Biotechnology, Lincoln, NE, USA) were used. Analysis and quantification was performed on an Odyssey Infrared Imaging system (LI-COR).

Soluble CD97 ELISA

Soluble CD97 (sCD97) in plasma was measured using a recently developed ELISA (32) based on 1B2 as capture Ab, biotinylated 1A2 as detection Ab, and streptavidin-conjugated HRP as enzyme. Blood from untreated wild-type, *Cd55*$^{-/-}$, and *Cd97*$^{-/-}$ mice or from recipient wild-type and *Cd55*$^{-/-}$ mice, 10 min after transfer of *Cd55*$^{-/-}$ immune cells, was collected in heparin, and plasma was obtained by centrifugation for 10 min at $16{,}200 \times g$ at 4°C. ELISA plates were coated overnight with 1 μg/ml 1B2 in PBS. Blocking was performed in 5% FCS and 0.01% Tween 20 in PBS. Plasma samples (50 μl) were added to the wells and incubated overnight at 4°C. Subsequently, wells were incubated with biotinylated 1A2 and streptavidin-conjugated HRP for 1 h at room temperature. After each step, samples were washed with 0.05% Tween 20 in PBS. Finally, tetramethylbenzidine was added as substrate, and the reaction was stopped with 2 N H_2SO_4. Absorbance was measured at 450 nm using 655 nm as a reference wavelength. Levels of sCD97 in plasma were calculated from a standard of recombinant mouse sCD97(EGF1,2,4)–mFc fusion protein (32) that was included on each plate.

Real-time quantitative PCR

Total RNA was extracted from peripheral blood leukocytes (PBLk) and transcribed into first-strand cDNA using Superscript II reverse transcriptase (Invitrogen, Carlsbad, CA). Real-time quantitative PCR was performed with the ABI Prism 7300 Sequence Detection System (Applied Biosystems, Foster City, CA) using SYBR Green Master Mix (Applied Biosystems) with an input of cDNA equal to 10 ng initial total RNA per reaction. Analysis was performed with Sequence Detection Software version 1.2.3 (Applied Biosystems). RNA expression of CD97 (forward primer 5′-CTGCCTC-ACCACAGCTACT-3′, reverse primer 5′-CTCAAGGGCTCT TCCCTT-TGT-3′) was normalized to hypoxanthine phosphoribosyltransferase (forward primer 5′-ATGGGAGGCCATCACATTGT-3′, reverse primer 5′-ATGTAATCCAGCAGGTCAGCAA-3′).

Statistical analysis

Differences between groups were calculated using unpaired *t* test or Mann–Whitney *U* test. Values are expressed as mean ± SD. A two-tailed *p* value <0.05 was considered to represent a significant difference.

Results

CD97 expression on immune cells is increased in Cd55$^{-/-}$ mice

Expression analysis by flow cytometry in wild-type mice revealed a broad distribution of CD97 on almost all leukocytes with, like in humans (33), highest expression levels found on myeloid cells (Fig. 1A). Notably, in mice lacking a functional *Cd55* gene, CD97 was significantly upregulated on all leukocytes, with the most prominent increase being found on cells in blood (Fig. 1A). This finding suggests that cell surface expression of CD97 is regulated by interaction with its ligand CD55.

Because flow cytometry allowed only detection of the extracellular part of CD97, the question arose whether expression differences observed in the absence of CD55 affects the whole receptor or only the α-chain. For example, it is conceivable that ligand binding induces release of the α-chain specifically, leaving expression of the membrane-spanning β-chain intact. Western blot analysis with Abs specific for the α- and β-chain of CD97 revealed that expression levels of both chains were increased in *Cd55$^{-/-}$* mice (Fig. 1B, *upper panel*). Quantification of the bands on the immunoblot showed that the α and β subunits of CD97 in *Cd55$^{-/-}$* mice were upregulated four times in PBLk and two times in splenocytes compared with wild-type mice (Fig. 1B, *lower panel*). These data imply that CD97 is predominantly expressed at the cell surface as a dimeric receptor, comprising both the α- and β-chain. We next tested whether CD55 deficiency leads to increased transcript levels of CD97. By quantitative PCR, we found comparable *Cd97* transcription in wild-type and *Cd55$^{-/-}$* leukocytes, indicating that modulation of CD97 protein expression through CD55 is regulated at the protein level (Fig. 1C).

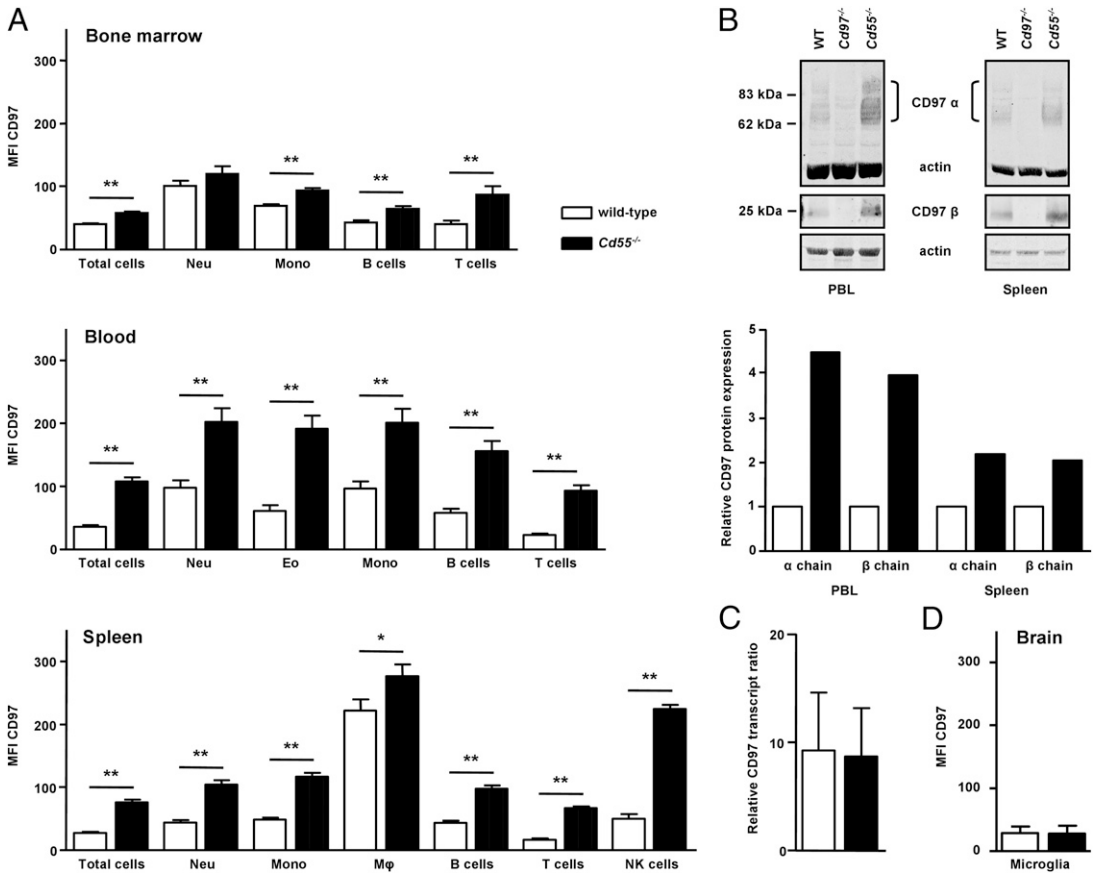

FIGURE 1. Lack of CD55 increases cell surface expression of both the α- and β-chain of CD97 on leukocytes. (**A**) Immune cells obtained from bone marrow, blood, and spleen of wild-type and *Cd55$^{-/-}$* mice were incubated with CD97 mAb 1B2 and analyzed by flow cytometry. The mean and SD of the geometric mean fluorescence intensity (MFI) of CD97 expression on total cells, neutrophils (Neu), eosinophils (Eo), monocytes (Mono), macrophages (Mφ), B cells, T cells, and NK cells (n = 6–19 mice) are shown. (**B**) Immune cells from blood and spleens were isolated from wild-type, *Cd97$^{-/-}$*, and *Cd55$^{-/-}$* mice. Western blot analysis of cell lysates using Abs specific for CD97 α- and β-chain was performed together with an actin control (*upper panel*). Bands on the shown immunoblot were quantified using Odyssey Imaging software (*lower panel*). The relative protein expression of CD97 compared with wild-type cells is shown. (**C**) Real-time quantitative PCR for CD97 on cDNA samples of PBLk of wild-type and *Cd55$^{-/-}$* mice. The mean and SD of CD97 transcript levels relative to hypoxanthine phosphoribosyltransferase (n = 4 mice) are shown. (**D**) CD11b^{+}CD45^{dim} microglia from brain specimens were analyzed for CD97 expression as in (A) (n = 5 mice). *$p < 0.05$, **$p < 0.005$.

Immune cell CD97 is reversibly regulated by CD55 expressed on stromal and hematopoietic cells

To corroborate the observation that CD55 regulates CD97 cell surface expression, we performed adoptive transfer experiments by i.v. injection of CD55-deficient splenocytes into wild-type recipients and vice versa. One day after the transfer, we assessed the cell surface expression of CD97 on the transferred cells present in blood (Fig. 2A) and spleen (data not shown). Wild-type immune cells that had been transferred into *Cd55*$^{-/-}$ mice showed an upregulation of CD97 expression within 24 h to levels comparable with CD55-deficient leukocytes. Conversely, when cells from CD55-deficient mice were transferred into an environment where CD55 was present, expression of CD97 on these leukocytes was downregulated to a level comparable to wild-type cells. Thus, surface expression of CD97 is reversibly regulated by the presence of CD55 in vivo.

Because CD55 is expressed widely throughout the body (34), we generated bone marrow–chimeric mice to study the role of CD55 on hematopoietic versus nonhematopoietic cells in regulating CD97 expression. Congenic wild-type and *Cd55*$^{-/-}$ recipient mice were lethally irradiated, followed by i.v. injection with *Cd55*$^{-/-}$ or wild-type bone marrow cells, respectively. Five weeks after reconstitution of the hematopoietic compartment, we analyzed the expression level of CD97 on PBLk of recipient mice. Levels of CD97 were comparable to wild-type mice in all conditions where CD55 was present (Fig. 2B). We concluded that CD55 of hematopoietic or stromal origin can regulate CD97 expression on immune cells.

De novo contact with CD55 leads to shedding of the α-chain and rapid downregulation of the β-chain of CD97 from the cell surface in vivo

To assess the kinetics of CD97 downregulation after ligation by CD55, we measured the expression of CD97 on *Cd55*$^{-/-}$ leukocytes at various time points after transfer to congenic wild-type mice. Within 5 min after the initial contact with wild-type cells bearing CD55 in the circulation, expression of CD97 on *Cd55*$^{-/-}$ leukocytes was already reduced by ~50% (Fig. 3A). At 20 min after transfer, CD97 expression was normalized to levels found on wild-type leukocytes (Fig. 3A).

To examine the fate of both the α- and β-chain of CD97 after ligation by CD55, we sorted transferred *Cd55*$^{-/-}$ cells from blood of both *Cd55*$^{-/-}$ and wild-type recipients 10 min after transfer. Western blot analysis with CD97 α- and β-chain–specific Abs revealed downregulation of both subunits after de novo contact with CD55. Quantification of the immunoblot confirmed an almost equal, 3-fold reduction in the amount of both chains, indicating that the two subunits of CD97 disappear after ligation with comparable kinetics (Fig. 3B).

Because of the two-subunit structure of CD97 and the presence of sCD97 in serum of wild-type mice (32), we wondered whether the α-chain is shed after ligation by CD55, followed by subsequent internalization and degradation of the β-chain. To test this possibility, we collected plasma of both *Cd55*$^{-/-}$ and wild-type recipients 10 min after transfer of *Cd55*$^{-/-}$ leukocytes into these mice. Using a sCD97-specific ELISA (32), we detected a low concentration of sCD97 in wild-type mice at steady state (Fig. 3C). Transfer of *Cd55*$^{-/-}$ leukocytes into wild-type recipients resulted in a significant increase in levels of circulating sCD97, indicating shedding of the α subunit after ligation of CD97 by CD55. In *Cd55*$^{-/-}$ mice, the level of sCD97 was below the detection limit and remained undetectable after transfer of *Cd55*$^{-/-}$ cells, further supporting the idea that ligation by CD55 is needed to process CD97.

CD55-induced downregulation of CD97 requires shear stress in vitro and in vivo

To study the mechanism by which CD55 is regulating CD97 cell surface expression, we tried to set up an in vitro system. We previously demonstrated physical interaction between CD97 and CD55 in coculture systems (5, 6, 29). Surprisingly, when studying *Cd55*$^{-/-}$ leukocytes cocultured with congenic wild-type blood cells, we observed no downregulation of CD97. We cocultured *Cd55*$^{-/-}$ leukocytes from spleen or blood with wild-type leukocytes or erythrocytes in different ratios and in the presence or absence of wild-type or *Cd55*$^{-/-}$ serum for 30 min until 48 h, but CD97 expression was downregulated in none of these conditions (data not shown). We concluded that the circumstances needed to regulate CD97 were not recapitulated properly in vitro. The difference could perhaps lie in the circulatory action of the blood, causing shear stress in vivo; this could trigger a conformational change resulting in CD55-mediated downregulation of CD97.

To test whether this shear stress model was viable, we attempted to recapitulate similar conditions in vitro. We cocultured CD55-

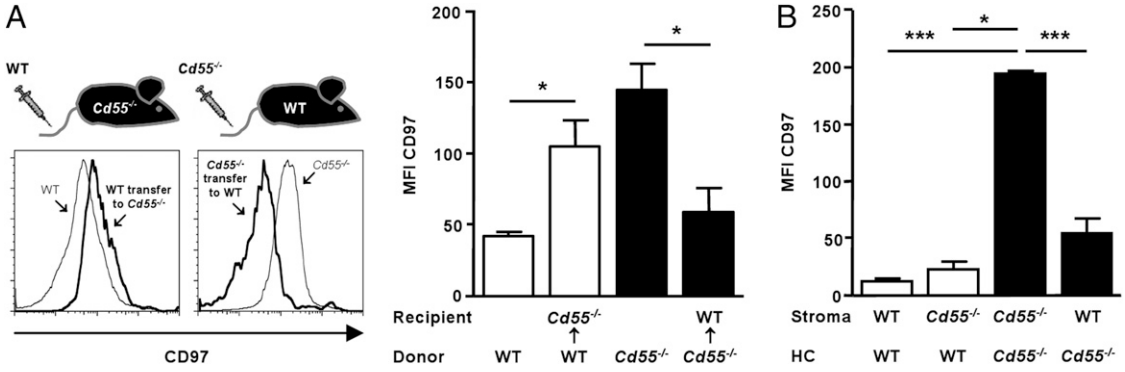

FIGURE 2. CD97 expression on leukocytes is reversibly regulated by CD55 on hematopoietic and nonhematopoietic cells. (**A**) Splenocytes from congenic wild-type and *Cd55*$^{-/-}$ mice were adoptively transferred to *Cd55*$^{-/-}$ and congenic wild-type recipients, respectively. PBLk were obtained 24 h after transfer and analyzed by flow cytometry for CD45.1, CD45.2, and CD97 expression. Shown are representative histograms and the mean and SD of the geometric mean fluorescence intensity (MFI) of CD97 expression on total donor leukocytes in blood of recipient mice compared with total leukocytes in wild-type and *Cd55*$^{-/-}$ mice (n = 3 mice). One of two independent experiments is shown. (**B**) *Cd55*$^{-/-}$ and congenic wild-type mice were lethally irradiated and reconstituted with 10×10^6 bone marrow–derived hematopoietic cells (HC) from congenic wild-type and *Cd55*$^{-/-}$ mice, respectively. Five weeks after reconstitution, PBLk were analyzed by flow cytometry for CD45.1, CD45.2, and CD97 expression. The mean and SD of the geometric MFI of CD97 expression on donor-derived total leukocytes are shown (n = 3–5 mice). *$p < 0.05$, ***$p < 0.0005$.

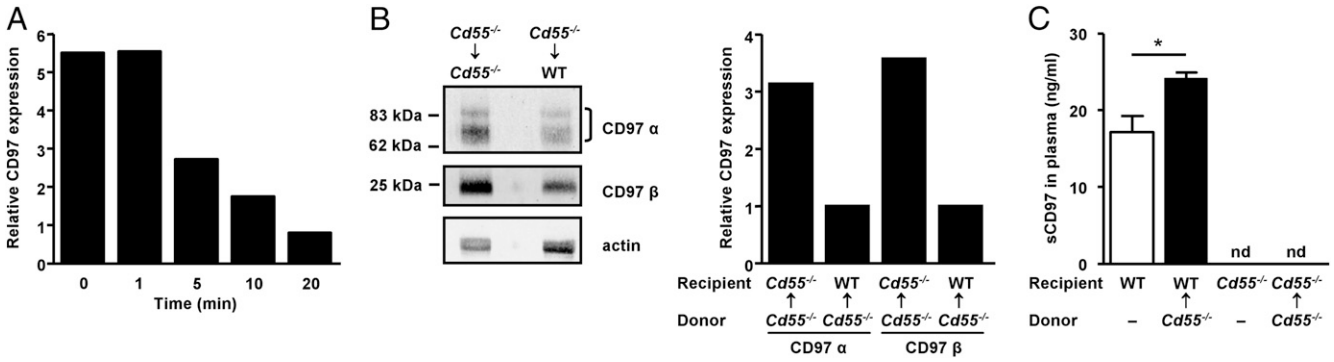

FIGURE 3. Ligation by CD55 in vivo results in CD97 α-chain shedding and β-chain downregulation. (**A**) Splenocytes from *Cd55*$^{-/-}$ mice were transferred into congenic wild-type mice by injection into the tail vein. At indicated time points, blood was collected from recipient mice, and CD97 expression was measured on transferred (CD45.2$^+$) and recipient (CD45.1$^+$) cells by flow cytometry. The relative expression of CD97 on transferred cells compared with host cells in the same mouse is shown for one of three independent experiments. (**B**) Splenocytes from *Cd55*$^{-/-}$ mice were labeled with CFSE and injected into the tail veins of *Cd55*$^{-/-}$ and wild-type mice. Blood was collected 10 min after transfer, erythrocytes were lysed, and CFSE$^+$ cells were sorted. Lysates of sorted cells from nine mice, derived from three experiments, were pooled and analyzed by Western blot using Abs specific for CD97 α- and β-chain together with an actin control (*left panel*). Bands on immunoblot shown were quantified using Odyssey Imaging software (*right panel*). The relative protein expression of CD97 on cells transferred into *Cd55*$^{-/-}$ mice compared with cells transferred into wild-type mice is shown. (**C**) Splenocytes from *Cd55*$^{-/-}$ mice were injected into the tail veins of *Cd55*$^{-/-}$ and wild-type mice. Blood was collected 10 min after transfer, and sCD97 was detected in plasma using a sandwich ELISA. Plasma levels of sCD97 in wild-type and *Cd55*$^{-/-}$ mice were analyzed for comparison. The mean ± SD of the amount of sCD97 in one of two independent experiments is shown (n = 3 mice). *$p < 0.05$. nd, Not detectable.

deficient splenocytes with wild-type blood while shaking at high speed. Shear stress in this model is heterogeneous, and for the current settings was ~30 dyne/cm^2 (35). After 4 h, CD97 expression on *Cd55*$^{-/-}$ cells was strongly reduced and comparable to that on wild-type leukocytes (Fig. 4A). Transferred *Cd55*$^{-/-}$ splenocytes were viable but slightly activated, as demonstrated by lower CD62L expression on transferred CD45.2$^+$ cells (data not shown). We previously showed that activated leukocytes express higher CD97 levels (36); therefore, cell activation should not have downregulated CD97 in our experiments. Analysis at earlier time points revealed that although somewhat slower than in vivo, CD97 was downregulated on *Cd55*$^{-/-}$ immune cells upon contact with wild-type blood cells within 1–2 h (Fig. 4B).

To corroborate our findings in a better-defined experimental setting, we used an MCR 501 Couette-type rheometer, where a nearly homogeneous shear stress field occurs in the fluid between two concentric cylinders, generated by their relative movement. We mixed *Cd55*$^{-/-}$ splenocytes with wild-type blood and applied a constant shear stress for 1 h. A shear stress of 1 dyne/cm^2, found in capillaries, was not sufficient to induce downregulation of CD97. In contrast, at a shear stress of 40 dyne/cm^2, which is representative for arteries, we observed that CD97 expression on transferred *Cd55*$^{-/-}$ cells was efficiently downregulated to wild-type levels (Fig. 4C).

We next investigated whether CD97 downregulation upon de novo ligation requires an intact circulation in vivo. As shown in Fig. 3A, *Cd55*$^{-/-}$ leukocytes rapidly downregulated CD97 after transfer into wild-type mice. To study regulation of CD97 expression in the absence of circulation, we pretreated wild-type recipient mice with heparin to prevent coagulation and sacrificed them immediately after adoptive transfer of *Cd55*$^{-/-}$ leukocytes, followed by cardiac puncture after 5 or 20 min. Under these

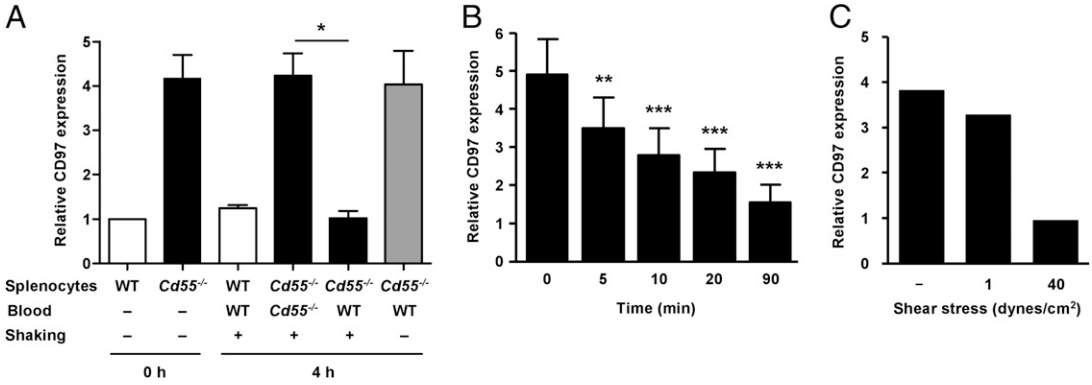

FIGURE 4. In vitro regulation of CD97 cell surface expression requires shear stress. (**A**) Splenocytes from *Cd55*$^{-/-}$ or congenic wild-type mice were cocultured for 4 h at room temperature with *Cd55*$^{-/-}$ or wild-type whole blood, applying rigorous agitation (white and black bars, shear ~ 30 dyne/cm^2) or not (gray bar). Immediately afterward, cells were analyzed for CD45.1, CD45.2, and CD97 expression by flow cytometry. Provided are the mean and SD of the relative expression of CD97 on the splenocytes, compared with wild-type splenocytes (0 h) or CD45.1$^+$ wild-type PBLk (4 h; n = 3). (**B**) Splenocytes from congenic *Cd55*$^{-/-}$ mice were cocultured at room temperature with wild-type whole blood, applying shear stress as in (A). At the indicated times, splenocytes were analyzed for CD97 expression, depicted here as mean and SD of relative expression compared with wild-type PBLk (n = 3–5). (**C**) Congenic wild-type whole blood was mixed with *Cd55*$^{-/-}$ splenocytes and exposed to a constant shear stress of 1 dyne/cm^2 or 40 dyne/cm^2 imposed by a rheometer. After 1 h, cells were harvested and analyzed by flow cytometry as described in (A). One of two comparable experiments is shown. *$p < 0.05$, **$p < 0.005$, ***$p < 0.0005$.

conditions, we found no reduction of CD97 cell surface expression, even after 20 min (Fig. 5). Erythrocytes express high levels of CD55, ensuring direct contact of CD97 on *Cd55*$^{-/-}$ leukocytes with its ligand, although there is no circulation. Treatment with heparin alone did not affect downregulation of CD97 expression on *Cd55*$^{-/-}$ leukocytes transferred into wild-type mice (data not shown). Together, these findings indicated that shear stress is necessary for the effective processing of CD97 by its ligand CD55. Consistent with this idea, we found that microglia in the brain that neither circulate nor are in contact with circulating blood cells have comparable levels of CD97 surface expression in wild-type and *Cd55*$^{-/-}$ mice (Fig. 1D).

De novo ligation of CD97 by its ligand CD55 does not induce ERK or protein kinase B/Akt signaling

In the classical model of agonist-selective desensitization, internalization of GPCRs results from effective receptor activation (37). Recent studies demonstrated that ectopic overexpression of CD97 in fibroblasts and epithelial cells, and constitutive expression of CD97 in prostate cancer cells stimulates ERK, protein kinase B (PKB)/Akt, and RhoA activation (22, 24). To explore the possibility that interaction with its ligand CD55 activates CD97 in leukocytes, we incubated CD55-deficient splenocytes with wild-type erythrocytes under rigorous agitation as described above. At 0, 5, 15, and 30 min, we harvested cells and probed lysates for ERK and PKB/Akt activation. We found no phosphorylation of ERK and PKB/Akt in splenocytes that had experienced CD97 ligation (Fig. 6). Moreover, RhoA was not activated upon de novo ligation of CD97 (data not shown); therefore, CD97 signaling pathways previously identified in tumor cells were not triggered by CD55 binding in leukocytes.

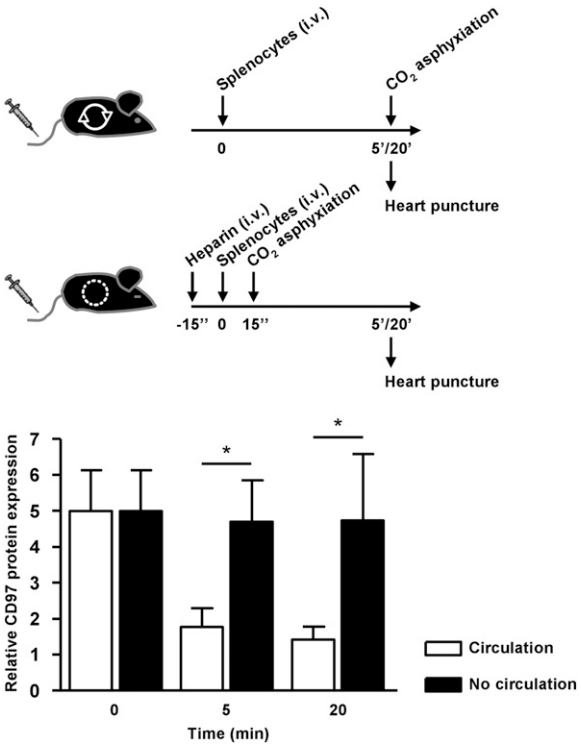

FIGURE 5. In vivo downregulation of CD97 upon CD55 contact requires blood circulation. One group of congenic wild-type mice was injected with *Cd55*$^{-/-}$ splenocytes by injection into the tail vein, followed by blood collection after 5 or 20 min. Another group of wild-type mice was administered with heparin, injected with *Cd55*$^{-/-}$ splenocytes, and sacrificed immediately thereafter. Blood was collected 5 and 20 min post mortem. CD97 expression was measured on transferred (CD45.2^{+}) and recipient (CD45.1^{+}) leukocytes by flow cytometry. Provided are the treatment scheme (*upper panel*) and the mean and SD of the relative expression of CD97 on transferred cells compared with host cells in the same mouse (*lower panel*). Data were pooled from three independent experiments (n = 6 mice). *$p < 0.05$.

Discussion

The identification of CD55 as a binding partner of CD97 in 1996 (5) demonstrated the ability of aGPCRs to interact with cellular ligands. Specificity and affinity of CD97 for CD55 is closely regulated by composition of the EGF domain region (6, 7, 29) and by individual amino acids that prevent CD55 binding by EMR2, a homolog of CD97 with 97% amino acid identity in the EGF domain region (7, 38). Despite cellular and molecular assays proving the interaction between CD97 and CD55 in humans and mice (5, 7, 29), it has been difficult to attain evidence that the two molecules interact in vivo. Importantly, EGF domain-specific Abs and recombinant CD55 do not activate known mediators of GPCR signaling (39). Recently, studies with gene-deficient mice functionally linked CD97 and CD55. First, mice lacking either CD97 or CD55 had a higher granulopoietic activity, resulting in increased numbers of circulating granulocytes (26, 40, 41). Second, the absence of CD97 or CD55 reduced disease activity in two experimental models of arthritis (42). In both cases, CD97 and CD55 knockout mice developed a highly similar phenotype. By their nature, these studies could establish only association but not prove causation. To our knowledge, our finding that CD97 surface expression on circulating leukocytes is continuously regulated by contact with CD55 provides the first direct evidence of an aGPCR interacting with its binding partner in vivo.

The physiologic function of the CD97–CD55 interaction presumably relates to the engagement of adhesive contacts between CD97^{+} immune cells and CD55^{+} stromal cells. It seems possible that CD97–CD55 contacts mediate the retention of leukocytes at specific tissue sites. For example, CD55^{high} synovial lining fibroblasts of rheumatoid arthritis synovial tissue are able to bind CD97-coupled fluorescent beads (43). A role of CD97 as receiver of local stromal and matrix adhesive codes would fit with its ability to engage with various ligands at low affinity. Besides CD55, CD97 binds the glycosaminoglycan dermatan sulfate, the integrin α5β1, and Thy-1/CD90 through different sites within the extracellular subunit (12, 13, 20). Similar characteristics have been reported for GPR56, an aGPCR expressed by neurons, various malignant cells, and cytotoxic lymphocytes (2, 44). GPR56 binds different ligands in man and mouse, including tissue transglutaminase 2 and collagen III (14, 19, 45). Defective expression of GPR56 on neurons disturbs the integrity of the pial basement membrane and the migration of developing neurons, resulting in a severe human brain malformation called bilateral frontoparietal polymicrogyria (46, 47). Intriguingly, all bilateral frontoparietal polymicrogyria–associated missense mutations identified to date are located at the extracellular region of GPR56 (46). Other examples of aGPCRs with a role in cell adhesion are Flamingo and Latrophilin, which coordinate cell orientation and tissue polarity in *Drosophila melanogaster* and *Caenorhabditis elegans*, respectively (48–51). The picture that arises from these studies is that aGPCRs facilitate the proper positioning of developing and motile cells in various organ systems via their extracellular modules.

CD97 and CD55 are abundantly expressed by all types of leukocytes (33, 52). Moreover, many epithelial cells express CD97, and CD55 is found on erythrocytes, endothelial cells, and stromal cells (11, 26, 53). This wide distribution raised the question of how uncontrolled clustering of leukocytes owing to homotypic or het-

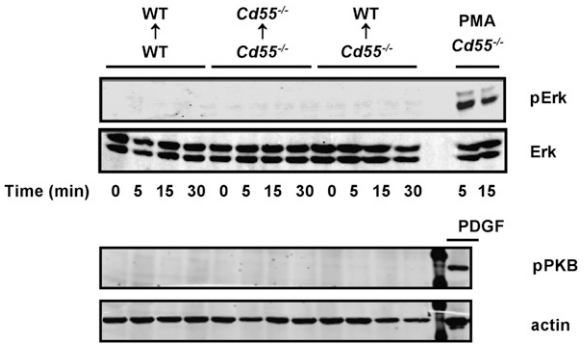

FIGURE 6. De novo interaction of CD97 with its ligand CD55 does not induce ERK or PKB/Akt signaling. $Cd55^{-/-}$ and wild-type splenocytes were mixed with either $Cd55^{-/-}$ or wild-type erythrocytes and shaken for 0, 5, 15, or 30 min. After erythrocyte lysis, splenocytes were collected in sample buffer and analyzed by Western blot with Abs specific for phosphorylated ERK and PKB/Akt. Full ERK or actin was analyzed for comparison of loading. As a positive control for ERK phosphorylation, splenocytes in the same experiment were stimulated with 100 ng/ml PMA. As a positive control for the pAkt Western blotting, lysate of platelet-derived growth factor (PDGF)-stimulated synovial fibroblasts was used. One of two independent experiments is shown.

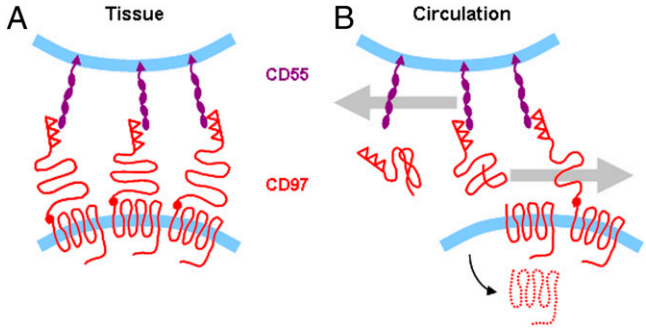

FIGURE 7. Consequences of the CD97–CD55 interaction in vivo. (**A**) In tissue, contacts between the aGPCR CD97 and the GPI-linked cell surface molecule CD55 can facilitate cell adhesion in situ. (**B**) In the circulation, CD97 expression is constantly downregulated by contact with CD55 on blood and stromal cells. For details on the model depicted here, see *Discussion*.

erotypic cellular CD97–CD55 contacts is prevented. Our data suggest that continuous downregulation of CD97 on circulating leukocytes upon contact with CD55, together with the rather low affinity of their interaction (K_D of 86 μM) (7), could prevent clustering or inappropriate binding to the endothelium. In line with this suggestion, we previously showed that CD97 and CD55 are dispensable for the extravasation of leukocytes from the blood stream (26, 36). Once inside the tissue, CD97 expression can increase and facilitate adhesion events through interaction with CD55. A unique aspect of the regulation of CD97 expression upon CD55 contact is the dependency on shear stress, both in vitro and in vivo. To our knowledge, this mechanism of downregulation of a GPCR is without precedent (Fig. 7). It remains to be shown whether the mechanism relates to the unique two-subunit structure, resulting from autocatalytic processing and reassociation of the protein precursor to almost unchanged appearance at the cell surface, which is a hallmark of most aGPCRs (3, 4). Based on our findings, it seems possible that the cleavage site in the GAIN domain functions as a molecular mechanical fracture device that confers a mechanism to terminate activity of the receptor.

It has been proposed that the two-subunit structure of aGPCRs functionally separates the adhesive extracellular subunit from the signaling seven-transmembrane subunit. Recent in vitro and in vivo studies with epithelial cells overexpressing CD97 have started to shed light on the signaling properties of the receptor. First, Becker et al. (22) and coworkers demonstrated an increase in membrane-associated β-catenin owing to PKB/Akt–GSK-3β signaling in transgenic *Villin-Cd97* mice that overexpress CD97 in intestinal epithelial cells. Second, Kelly et al. (24) showed that in prostate cancer cells, CD97 signals through ERK, PKB/Akt, and RhoA activation. Notably, signaling has not been attributed to receptor ligation in these studies, and Ward et al. (24, 54) demonstrated that CD97 in a ligand-independent manner regulates signaling of lysophosphatidic acid receptor 1. We tested whether de novo ligation by CD55 would stimulate CD97 signaling, but found no evidence that ERK, PKB/Akt, or RhoA are activated, although our in vitro experimental settings mimic in vivo events closely. Whereas our experiments do not exclude signaling, perhaps mediated by signaling molecules other than the ones tested, it also seems possible that CD55 binding not at all triggers CD97 signaling but solely mediates adhesive contacts. This question will need to be addressed in future studies using robust and specific readouts for CD97 signaling.

As a consequence of the two-subunit structure of aGPCRs, the two chains can behave as independent proteins as has been shown by studies with transfected cell lines for latrophilin and EMR2 (55, 56). In this study, we failed to demonstrate an independent existence of the transmembrane β-chain of CD97 after dissociation from the extracellular α-chain. Upon CD55-induced shedding of the α-chain in vivo, the β-chain was downregulated within minutes to the same extent, most likely via internalization and subsequent degradation. The orchestration of this process remains to be addressed.

Another question relates to the possible roles of the CD97 α-chain in the circulation. Shed ectodomains of transmembrane proteins can remain stable and active in solution, thereby regulating various biological processes (57). Interestingly, the α-chain of human CD97 can act as a potent chemoattractant for human endothelial cells and as a proangiogenic factor (13), manifesting its potential biological activity at distant sites. Lack of sCD97 in CD55 knockout mice suggests that CD55 contact-mediated release is the major source of CD97 α-chain present in plasma.

In summary, we show that ligation of the aGPCR CD97 on circulating blood cells results in rapid downregulation of the receptor, probably to restrict cell adhesion to tissue sites. The de novo ligation model that we present can facilitate future studies on the working mechanism of aGPCRs.

Acknowledgments

We thank Berend Hooibrink for performing cell sorts, Mark Hoogenboezem for performing RhoA pull-down assay, and Profs. Claude Libert, Joost C.M. Meijers, and Ghislain Opdenakker for experimental advice and helpful discussions.

Disclosures

The authors have no financial conflicts of interest.

References

1. Lagerström, M. C., and H. B. Schiöth. 2008. Structural diversity of G protein-coupled receptors and significance for drug discovery. *Nat. Rev. Drug Discov.* 7: 339–357.
2. Yona, S., H. H. Lin, W. O. Siu, S. Gordon, and M. Stacey. 2008. Adhesion-GPCRs: emerging roles for novel receptors. *Trends Biochem. Sci.* 33: 491–500.
3. Lin, H. H., G. W. Chang, J. Q. Davies, M. Stacey, J. Harris, and S. Gordon. 2004. Autocatalytic cleavage of the EMR2 receptor occurs at a conserved G protein-coupled receptor proteolytic site motif. *J. Biol. Chem.* 279: 31823–31832.

4. Araç, D., A. A. Boucard, M. F. Bolliger, J. Nguyen, S. M. Soltis, T. C. Südhof, and A. T. Brunger. 2012. A novel evolutionarily conserved domain of cell-adhesion GPCRs mediates autoproteolysis. *EMBO J.* 31: 1364–1378.
5. Hamann, J., B. Vogel, G. M. W. van Schijndel, and R. A. W. van Lier. 1996. The seven-span transmembrane receptor CD97 has a cellular ligand (CD55, DAF). *J. Exp. Med.* 184: 1185–1189.
6. Hamann, J., C. Stortelers, E. Kiss-Toth, B. Vogel, W. Eichler, and R. A. W. van Lier. 1998. Characterization of the CD55 (DAF)-binding site on the seven-span transmembrane receptor CD97. *Eur. J. Immunol.* 28: 1701–1707.
7. Lin, H. H., M. Stacey, C. Saxby, V. Knott, Y. Chaudhry, D. Evans, S. Gordon, A. J. McKnight, P. Handford, and S. Lea. 2001. Molecular analysis of the epidermal growth factor-like short consensus repeat domain-mediated protein-protein interactions: dissection of the CD97-CD55 complex. *J. Biol. Chem.* 276: 24160–24169.
8. Abbott, R. J., I. Spendlove, P. Roversi, H. Fitzgibbon, V. Knott, P. Teriete, J. M. McDonnell, P. A. Handford, and S. M. Lea. 2007. Structural and functional characterization of a novel T cell receptor co-regulatory protein complex, CD97-CD55. *J. Biol. Chem.* 282: 22023–22032.
9. Hamann, J., W. Eichler, D. Hamann, H. M. Kerstens, P. J. Poddighe, J. M. Hoovers, E. Hartmann, M. Strauss, and R. A. van Lier. 1995. Expression cloning and chromosomal mapping of the leukocyte activation antigen CD97, a new seven-span transmembrane molecule of the secretion receptor superfamily with an unusual extracellular domain. *J. Immunol.* 155: 1942–1950.
10. Gray, J. X., M. Haino, M. J. Roth, J. E. Maguire, P. N. Jensen, A. Yarme, M. A. Stetler-Stevenson, U. Siebenlist, and K. Kelly. 1996. CD97 is a processed, seven-transmembrane, heterodimeric receptor associated with inflammation. *J. Immunol.* 157: 5438–5447.
11. Jaspars, L. H., W. Vos, G. Aust, R. A. Van Lier, and J. Hamann. 2001. Tissue distribution of the human CD97 EGF-TM7 receptor. *Tissue Antigens* 57: 325–331.
12. Stacey, M., G. W. Chang, J. Q. Davies, M. J. Kwakkenbos, R. D. Sanderson, J. Hamann, S. Gordon, and H. H. Lin. 2003. The epidermal growth factor-like domains of the human EMR2 receptor mediate cell attachment through chondroitin sulfate glycosaminoglycans. *Blood* 102: 2916–2924.
13. Wang, T., Y. Ward, L. H. Tian, R. Lake, L. Guedez, W. G. Stetler-Stevenson, and K. Kelly. 2005. CD97, an adhesion receptor on inflammatory cells, stimulates angiogenesis through binding integrin counterreceptors on endothelial cells. *Blood* 105: 2836–2844.
14. Xu, L., S. Begum, J. D. Hearn, and R. O. Hynes. 2006. GPR56, an atypical G protein-coupled receptor, binds tissue transglutaminase, TG2, and inhibits melanoma tumor growth and metastasis. *Proc. Natl. Acad. Sci. USA* 103: 9023–9028.
15. Park, D., A. C. Tosello-Trampont, M. R. Elliott, M. Lu, L. B. Haney, Z. Ma, A. L. Klibanov, J. W. Mandell, and K. S. Ravichandran. 2007. BAI1 is an engulfment receptor for apoptotic cells upstream of the ELMO/Dock180/Rac module. *Nature* 450: 430–434.
16. Das, S., K. A. Owen, K. T. Ly, D. Park, S. G. Black, J. M. Wilson, C. D. Sifri, K. S. Ravichandran, P. B. Ernst, and J. E. Casanova. 2011. Brain angiogenesis inhibitor 1 (BAI1) is a pattern recognition receptor that mediates macrophage binding and engulfment of Gram-negative bacteria. *Proc. Natl. Acad. Sci. USA* 108: 2136–2141.
17. Bolliger, M. F., D. C. Martinelli, and T. C. Südhof. 2011. The cell-adhesion G protein-coupled receptor BAI3 is a high-affinity receptor for C1q-like proteins. *Proc. Natl. Acad. Sci. USA* 108: 2534–2539.
18. Silva, J. P., V. G. Lelianova, Y. S. Ermolyuk, N. Vysokov, P. G. Hitchen, O. Berninghausen, M. A. Rahman, A. Zangrandi, S. Fidalgo, A. G. Tonevitsky, et al. 2011. Latrophilin 1 and its endogenous ligand Lasso/teneurin-2 form a high-affinity transsynaptic receptor pair with signaling capabilities. *Proc. Natl. Acad. Sci. USA* 108: 12113–12118.
19. Luo, R., S. J. Jeong, Z. Jin, N. Strokes, S. Li, and X. Piao. 2011. G protein-coupled receptor 56 and collagen III, a receptor-ligand pair, regulates cortical development and lamination. *Proc. Natl. Acad. Sci. USA* 108: 12925–12930.
20. Wandel, E., A. Saalbach, D. Sittig, C. Gebhardt, and G. Aust. 2012. Thy-1 (CD90) is an interacting partner for CD97 on activated endothelial cells. *J. Immunol.* 188: 1442–1450.
21. Koirala, S., Z. Jin, X. Piao, and G. Corfas. 2009. GPR56-regulated granule cell adhesion is essential for rostral cerebellar development. *J. Neurosci.* 29: 7439–7449.
22. Becker, S., E. Wandel, M. Wobus, R. Schneider, S. Amasheh, D. Sittig, C. Kerner, R. Naumann, J. Hamann, and G. Aust. 2010. Overexpression of CD97 in intestinal epithelial cells of transgenic mice attenuates colitis by strengthening adherens junctions. *PLoS ONE* 5: e8507.
23. Pierce, K. L., R. T. Premont, and R. J. Lefkowitz. 2002. Seven-transmembrane receptors. *Nat. Rev. Mol. Cell Biol.* 3: 639–650.
24. Ward, Y., R. Lake, J. J. Yin, C. D. Heger, M. Raffeld, P. K. Goldsmith, M. Merino, and K. Kelly. 2011. LPA receptor heterodimerizes with CD97 to amplify LPA-initiated RHO-dependent signaling and invasion in prostate cancer cells. *Cancer Res.* 71: 7301–7311.
25. Lin, F., Y. Fukuoka, A. Spicer, R. Ohta, N. Okada, C. L. Harris, S. N. Emancipator, and M. E. Medof. 2001. Tissue distribution of products of the mouse decay-accelerating factor (DAF) genes. Exploitation of a Daf1 knock-out mouse and site-specific monoclonal antibodies. *Immunology* 104: 215–225.
26. Veninga, H., S. Becker, R. M. Hoek, M. Wobus, E. Wandel, J. van der Kaa, M. van der Valk, A. F. de Vos, H. Haase, B. Owens, et al. 2008. Analysis of CD97 expression and manipulation: antibody treatment but not gene targeting curtails granulocyte migration. *J. Immunol.* 181: 6574–6583.
27. Rops, A. L., C. W. Jacobs, P. C. Linssen, J. B. Boezeman, J. F. Lensen, T. J. Wijnhoven, L. P. van den Heuvel, T. H. van Kuppevelt, J. van der Vlag, and J. H. Berden. 2007. Heparan sulfate on activated glomerular endothelial cells and exogenous heparinoids influence the rolling and adhesion of leucocytes. *Nephrol. Dial. Transplant.* 22: 1070–1077.
28. Cheng, C., F. Helderman, D. Tempel, D. Segers, B. Hierck, R. Poelmann, A. van Tol, D. J. Duncker, D. Robbers-Visser, N. T. Ursem, et al. 2007. Large variations in absolute wall shear stress levels within one species and between species. *Atherosclerosis* 195: 225–235.
29. Hamann, J., C. van Zeventer, A. Bijl, C. Molenaar, K. Tesselaar, and R. A. van Lier. 2000. Molecular cloning and characterization of mouse CD97. *Int. Immunol.* 12: 439–448.
30. Leemans, J. C., A. A. te Velde, S. Florquin, R. J. Bennink, K. de Bruin, R. A. van Lier, T. van der Poll, and J. Hamann. 2004. The epidermal growth factor-seven transmembrane (EGF-TM7) receptor CD97 is required for neutrophil migration and host defense. *J. Immunol.* 172: 1125–1131.
31. Sedgwick, J. D., S. Schwender, H. Imrich, R. Dörries, G. W. Butcher, and V. ter Meulen. 1991. Isolation and direct characterization of resident microglial cells from the normal and inflamed central nervous system. *Proc. Natl. Acad. Sci. USA* 88: 7438–7442.
32. de Groot, D. M., G. Vogel, J. Dulos, L. Teeuwen, K. Stebbins, J. Hamann, B. M. Owens, H. van Eenennaam, E. Bos, and A. M. Boots. 2009. Therapeutic antibody targeting of CD97 in experimental arthritis: the role of antigen expression, shedding, and internalization on the pharmacokinetics of anti-CD97 monoclonal antibody 1B2. *J. Immunol.* 183: 4127–4134.
33. Kop, E. N., M. Matmati, W. Pouwels, G. Leclercq, P. P. Tak, and J. Hamann. 2009. Differential expression of CD97 on human lymphocyte subsets and limited effect of CD97 antibodies on allogeneic T-cell stimulation. *Immunol. Lett.* 123: 160–168.
34. Lublin, D. M., and J. P. Atkinson. 1989. Decay-accelerating factor: biochemistry, molecular biology, and function. *Annu. Rev. Immunol.* 7: 35–58.
35. Ley, K., E. Lundgren, E. Berger, and K. E. Arfors. 1989. Shear-dependent inhibition of granulocyte adhesion to cultured endothelium by dextran sulfate. *Blood* 73: 1324–1330.
36. Veninga, H., D. M. de Groot, N. McCloskey, B. M. Owens, M. C. Dessing, J. S. Verbeek, S. Nourshargh, H. van Eenennaam, A. M. Boots, and J. Hamann. 2011. CD97 antibody depletes granulocytes in mice under conditions of acute inflammation via a Fc receptor-dependent mechanism. *J. Leukoc. Biol.* 89: 413–421.
37. Kelly, E., C. P. Bailey, and G. Henderson. 2008. Agonist-selective mechanisms of GPCR desensitization. *Br. J. Pharmacol.* 153(Suppl 1): S379–S388.
38. Lin, H. H., M. Stacey, J. Hamann, S. Gordon, and A. J. McKnight. 2000. Human EMR2, a novel EGF-TM7 molecule on chromosome 19p13.1, is closely related to CD97. *Genomics* 67: 188–200.
39. Kwakkenbos, M. J., E. N. Kop, M. Stacey, M. Matmati, S. Gordon, H. H. Lin, and J. Hamann. 2004. The EGF-TM7 family: a postgenomic view. *Immunogenetics* 55: 655–666.
40. Wang, T., L. Tian, M. Haino, J. L. Gao, R. Lake, Y. Ward, H. Wang, U. Siebenlist, P. M. Murphy, and K. Kelly. 2007. Improved antibacterial host defense and altered peripheral granulocyte homeostasis in mice lacking the adhesion class G protein receptor CD97. *Infect. Immun.* 75: 1144–1153.
41. Veninga, H., R. M. Hoek, A. F. de Vos, A. M. de Bruin, F. Q. An, T. van der Poll, R. A. van Lier, M. E. Medof, and J. Hamann. 2011. A novel role for CD55 in granulocyte homeostasis and anti-bacterial host defense. *PLoS ONE* 6: e24431.
42. Hoek, R. M., D. de Launay, E. N. Kop, A. S. Yilmaz-Elis, F. Lin, K. A. Reedquist, J. S. Verbeek, M. E. Medof, P. P. Tak, and J. Hamann. 2010. Deletion of either CD55 or CD97 ameliorates arthritis in mouse models. *Arthritis Rheum.* 62: 1036–1042.
43. Kop, E. N., M. J. Kwakkenbos, G. J. D. Teske, M. C. Kraan, T. J. Smeets, M. Stacey, H. H. Lin, P. P. Tak, and J. Hamann. 2005. Identification of the epidermal growth factor-TM7 receptor EMR2 and its ligand dermatan sulfate in rheumatoid synovial tissue. *Arthritis Rheum.* 52: 442–450.
44. Peng, Y. M., M. D. van de Garde, K. F. Cheng, P. A. Baars, E. B. Remmerswaal, R. A. van Lier, C. R. Mackay, H. H. Lin, and J. Hamann. 2011. Specific expression of GPR56 by human cytotoxic lymphocytes. *J. Leukoc. Biol.* 90: 735–740.
45. Chiang, N. Y., C. C. Hsiao, Y. S. Huang, H. Y. Chen, I. J. Hsieh, G. W. Chang, and H. H. Lin. 2011. Disease-associated GPR56 mutations cause bilateral frontoparietal polymicrogyria via multiple mechanisms. *J. Biol. Chem.* 286: 14215–14225.
46. Piao, X., R. S. Hill, A. Bodell, B. S. Chang, L. Basel-Vanagaite, R. Straussberg, W. B. Dobyns, B. Qasrawi, R. M. Winter, A. M. Innes, et al. 2004. G protein-coupled receptor-dependent development of human frontal cortex. *Science* 303: 2033–2036.
47. Li, S., Z. Jin, S. Koirala, L. Bu, L. Xu, R. O. Hynes, C. A. Walsh, G. Corfas, and X. Piao. 2008. GPR56 regulates pial basement membrane integrity and cortical lamination. *J. Neurosci.* 28: 5817–5826.
48. Usui, T., Y. Shima, Y. Shimada, S. Hirano, R. W. Burgess, T. L. Schwarz, M. Takeichi, and T. Uemura. 1999. Flamingo, a seven-pass transmembrane cadherin, regulates planar cell polarity under the control of Frizzled. *Cell* 98: 585–595.
49. Chen, W. S., D. Antic, M. Matis, C. Y. Logan, M. Povelones, G. A. Anderson, R. Nusse, and J. D. Axelrod. 2008. Asymmetric homotypic interactions of the atypical cadherin flamingo mediate intercellular polarity signaling. *Cell* 133: 1093–1105.
50. Langenhan, T., S. Prömel, L. Mestek, B. Esmaeili, H. Waller-Evans, C. Hennig, Y. Kohara, L. Avery, I. Vakonakis, R. Schnabel, and A. P. Russ. 2009. Latrophilin

signaling links anterior-posterior tissue polarity and oriented cell divisions in the C. elegans embryo. *Dev. Cell* 17: 494–504.
51. Steimel, A., L. Wong, E. H. Najarro, B. D. Ackley, G. Garriga, and H. Hutter. 2010. The Flamingo ortholog FMI-1 controls pioneer-dependent navigation of follower axons in C. elegans. *Development* 137: 3663–3673.
52. Nickells, M. W., J. I. Alvarez, D. M. Lublin, and J. P. Atkinson. 1994. Characterization of DAF-2, a high molecular weight form of decay-accelerating factor (DAF; CD55), as a covalently cross-linked dimer of DAF-1. *J. Immunol.* 152: 676–685.
53. Nicholson-Weller, A., and C. E. Wang. 1994. Structure and function of decay accelerating factor CD55. *J. Lab. Clin. Med.* 123: 485–491.
54. Ward, Y., R. Lake, P. L. Martin, K. Killian, P. Salerno, T. Wang, P. Meltzer, M. Merino, S. Y. Cheng, M. Santoro, et al. 2012. CD97 amplifies LPA receptor signaling and promotes thyroid cancer progression in a mouse model. *Oncogene.* In press.
55. Volynski, K. E., J. P. Silva, V. G. Lelianova, M. Atiqur Rahman, C. Hopkins, and Y. A. Ushkaryov. 2004. Latrophilin fragments behave as independent proteins that associate and signal on binding of LTX(N4C). *EMBO J.* 23: 4423–4433.
56. Huang, Y. S., N. Y. Chiang, C. H. Hu, C. C. Hsiao, K. F. Cheng, W. P. Tsai, S. Yona, M. Stacey, S. Gordon, G. W. Chang, and H. H. Lin. 2012. Activation of myeloid cell-specific adhesion class G protein-coupled receptor EMR2 via ligation-induced translocation and interaction of receptor subunits in lipid raft microdomains. *Mol. Cell. Biol.* 32: 1408–1420.
57. Huovila, A. P., A. J. Turner, M. Pelto-Huikko, I. Kärkkäinen, and R. M. Ortiz. 2005. Shedding light on ADAM metalloproteinases. *Trends Biochem. Sci.* 30: 413–422.